ELSEVIER

Journal of Alloys and Compounds 216 (1994) 177–182

Journal of ALLOYS AND COMPOUNDS

Bonding and interlayer charge transfer in the solid state compound $Na_{1.9}Cu_2Se_2Cu_2O$

Gerardo Chacon, Xiangyun Long[1], Chong Zheng*

Department of Chemistry, Northern Illinois University, DeKalb, IL 60115, USA

Received 4 April 1994; in final form 20 May 1994

Abstract

The bonding and electronic structure of an electron-deficient solid $Na_{1.9}Cu_2Se_2Cu_2O$ are analyzed with the extended Hückel tight-binding method. This solid consists of three kinds of layers: a Cu_2O layer with square-coordinated oxygen atoms, an anti-PbO type Cu_2Se_2 layer, and a cationic Na layer. The Cu_2O layer has a closed-shell electronic structure, whereas the Cu_2Se_2 layer needs two more electrons per Cu_2Se_2 to complete a closed-shell configuration. Thus charge transfer takes place mainly from the Na layer to the Cu_2Se_2 layer. The holes created by the incomplete occupancy at the Na sites reside in the Cu_2Se_2 layer.

Keywords: Bonding; Electronic structure; Interlayer charge transfer

1. Introduction

Charge transfer in the solid state may play an important role in determining the physical properties of the materials. For example, the charge disproportionation of Cu atoms in the conduction and reservoir layers, $Cu^{2+} + Cu^{2+} \rightarrow Cu^{1+} + Cu^{3+}$, was proposed to be responsible for the unusually high superconducting temperature in cuprate superconductors [1]. Many members of the $ThCr_2Si_2$ and related $CaBe_2Ge_2$ families also exhibit interesting physical properties, such as heavy fermion and intriguing magnetic behaviors [2,3]. The $CaBe_2Ge_2$ type solids consist of donor and acceptor layers in which charge transfer takes place as a consequence of different bonding patterns in individual layers [4].

Recently, a new solid, $Na_{1.9}Cu_2Se_2Cu_2O$, was synthesized in Kanatzidis's group [5]. The solid consists of three types of layers (see **1**): the Cu_2O layer (anti-CuO_2 type), the Cu_2Se_2 and the Na layers. In the square Cu_2O layer (see **2**), each Cu atom is located on the edge of the square and linearly coordinated to two oxygen atoms (Cu-O: 1.96 Å). The Cu–Cu distance is 2.77 Å, much longer than a typical $Cu(d^{10})$–$Cu(d^{10})$ bond distance of 2.35–2.45 Å in discrete molecules [6], and even longer than the Cu–Cu contact of 2.56 Å in Cu metal. The Se atom in the Cu_2Se_2 layer is 3.88 Å away from the oxygen atom in the Cu_2O layer. Thus there is little interaction between these two layers. The coordination of the oxygen atom to four transition metal atoms in the square-planar geometry occurs in several other types of solids, such as in NbO, $Sc_{0.75}Zn_{1.25}Mo_4O_7$, and $ZnMo_4O_8$ [7–11]. It is also observed in the Pb_2O_2 sheet of the high temperature superconductor $[(PbO)_2Cu]Y_{1-x}Ca_xSr_2Cu_2O_{6+\delta}$, although the interaction with other layers makes a higher coordination number for oxygen atoms in this solid [12]. It is therefore important that we understand the electronic driving force for this bonding geometry.

The other layer is the anti-PbO type Cu_2Se_2 sheet, **3**. It consists of the edge sharing $CuSe_4$ tetrahedra extending in two dimensions. This type occurs also in the $ThCr_2Si_2$ and $CaBe_2Ge_2$ families, and their bonding pattern has been studied [4,13]. The Cu–Se distance is 2.48 Å, a little longer than the sum of the covalent radii of Cu and Se (1.17 + 1.16 Å). But it is shorter than the Cu–Se distance 2.55 Å in an isolated NaCuSe compound in the tetragonal PbFCl structure [14].

The Na layer acts as electron donors, giving 1.9 electrons per unit to other layers. It is not obvious, however, which layer, the Cu_2O or the Cu_2Se_2 layer, is the more likely recipient.

*Corresponding author.

[1]Present address: Department of Chemistry, Central South University, Hunan 410083, China.

SSDI 0925-8388(94)01284-O

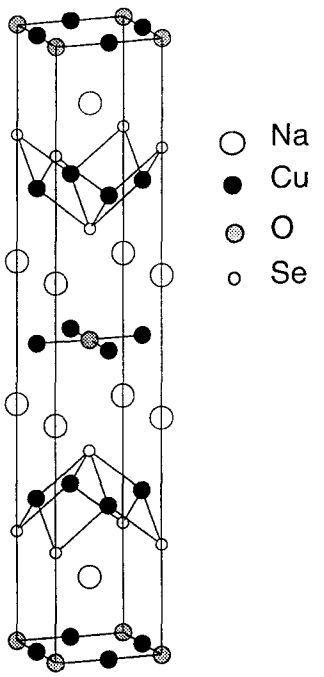

1

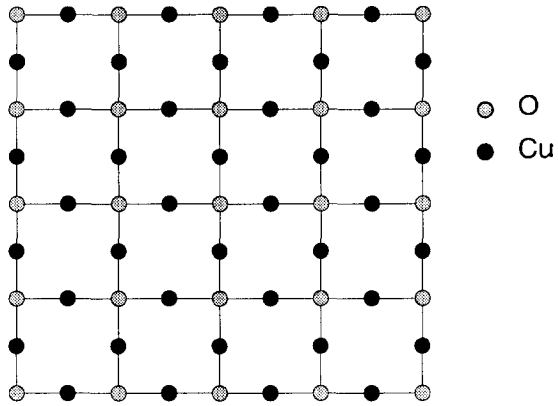

2

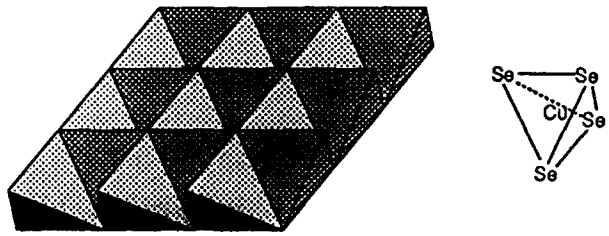

3

$Na_{1.9}Cu_2Se_2Cu_2O$ is metallic. Kanatzidis and his co-workers have proposed that it is due to the holes created by the incomplete occupancy at the Na sites (1.9 Na atoms instead of two). If so, where do the holes reside, in the Cu_2O layer or in the Cu_2Se_2 layer? In this contribution, we analyze the bonding and electronic structure of this compound and address the above issues. The computational tool used is the tight-binding extended Hückel method. The parameters used in this method are listed in the Appendix.

2. The Cu_2O layer

We first analyze the electronic structure of the Cu_2O layer (see **2**). We can formally assign the oxidation state of Cu as Cu^{+1} (d^{10}) and that of O as O^{2-}. Thus all oxygen orbitals (2s and 2p) are filled. Each copper atom is linearly coordinated to two oxygen atoms. Many examples of this linear X–M(d^{10})–X coordination exist, both in discrete molecules [15–19] and in the solid state [8,20,21]. The electronic structure of a d^{10} transition metal is well known [6,22], and is discussed briefly in the following.

The schematic interaction diagram of an O–Cu–O motif is shown in **4**. On the left side, Cu^{+1} has 10 d valence electrons, 6 of them in the t_{2g} set, and 4 in the e_g set. On the right-hand side, two oxygen sp hybrids pointing towards the Cu atoms form in-phase and out-of-phase combinations. These two hybrid orbitals interact with the two Cu sp orbitals most strongly. This interaction will stabilize the filled oxygen hybrids and destabilize the Cu sp orbitals. Similarly, the two oxygen p orbitals (p_x and p_y) are stabilized by two of the t_{2g} orbitals (*xy* and *xz*). These two t_{2g} orbitals would be Cu–O antibonding, but they mix with the Cu p_x and p_y orbitals to become weakly antibonding. The remaining three Cu orbitals, one t_{2g} (*yz*) and two e_g orbitals, are thus essentially non-bonding. The Cu d orbitals accommodate 10 electrons. Thus a linearly coordinated Cu^{+1} is in a closed-shell configuration. The main stabilization in this coordination geometry comes from the interaction between the oxygen and Cu sp hybrid orbitals.

The square coordination of oxygen occurs in several types of solids. The most prominent example is perhaps NbO [7,8], others include $Sc_{0.75}Zn_{1.25}Mo_4O_7$ [9,10],

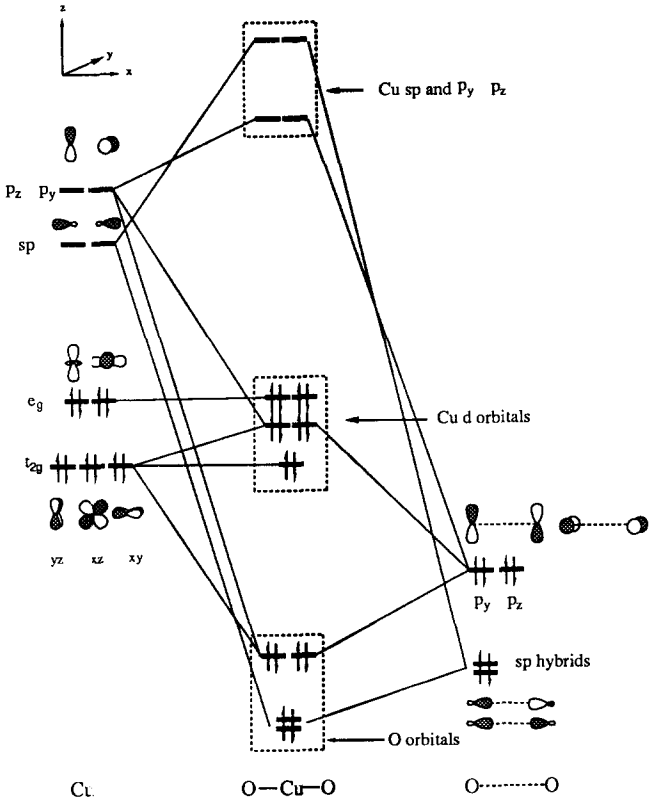

4

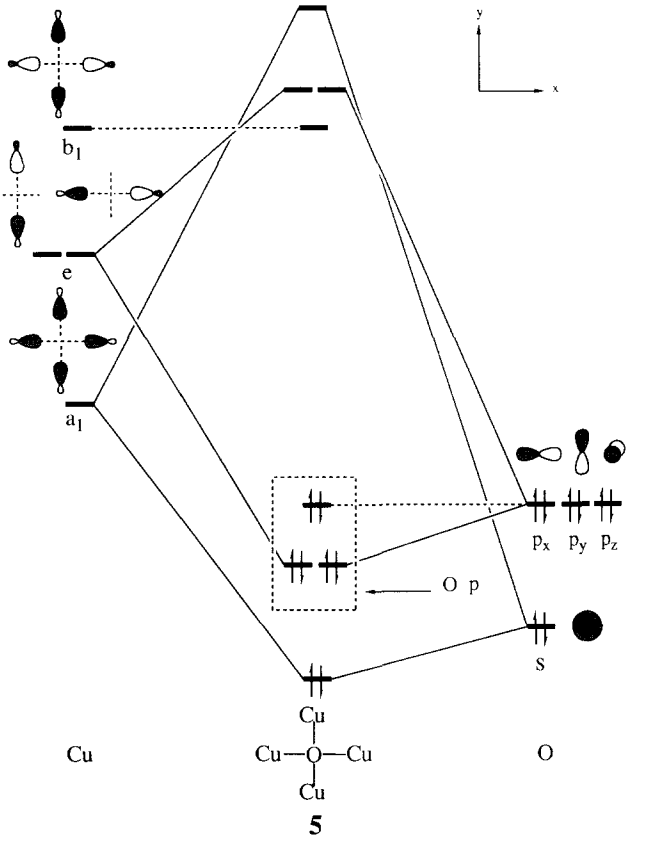

5

$ZnMo_8O_{10}$, $LiMo_8O_{10}$ [11], and the Pb_2O_2 layer in the superconductor $[(PbO)_2Cu]Y_{1-x}Ca_xSr_2Cu_2O_{6+\delta}$ [12]. The molecular example, however, is rare. The first one was reported by Rambo et al. in an unusual compound $(NBu^n_4)_2[V_4O(edt)_2Cl_8]$ [23]. The bonding pattern in both the solid and the molecule has been investigated by several authors [23,24].

We can also view the stabilization at the oxygen sites. From **4**, we know that each Cu has two sp hybrid orbitals pointing towards the two neighboring oxygen atoms. Thus each oxygen is surrounded by four Cu sp hybrids. These four hybrids form four cyclobutadienoid symmetry-adapted molecular orbitals on the left side of **5**. The a_1 orbital interacts with oxygen 2s; and e with oxygen p_x and p_y on the right side of **5**. Oxygen s and p_x, p_y are then stabilized. Although in **5** the oxygen p_z orbital is non-bonding, it is actually stabilized through the interaction with the Cu t_{2g} orbitals (see **4**). Therefore, a square-coordinated oxygen atom with filled orbitals (O^{2-}) is energetically stable, because all the oxygen orbitals are stabilized by the empty Cu sp hybrid and p orbitals.

In the solid state, each orbital develops into a band. But we can still ask how much a particular orbital described above contributes to the total density of states (DOS). Fig. 1(a) is the band structure of the two-dimensional Cu_2O layer. The bands immediately below the Fermi level (ϵ_F) are mostly Cu t_{2g} and e_g orbitals, which are Cu–O non-bonding or weakly antibonding. Fig. 1(b,c) shows the composition of these bands. Below the Fermi level, Cu d orbitals contribute greatly to DOS. Above the Fermi level, the bands are mostly Cu sp, p_y and p_z orbitals, and should be Cu–O antibonding. The crystal orbital overlap population (COOP) curve in Fig. 1(d) (solid line) confirms this; the states below the Fermi level are mostly Cu–O bonding or weakly antibonding; those above the Fermi level are antibonding.

The weakly Cu–O antibonding character immediately below the Fermi level is also partly due to the Cu–Cu contact and other secondary interactions, but the essential features in **4** and **5** are preserved. The Cu–Cu contact is antibonding due to the filled d block, but the mixing with the sp hybrids, p_x and p_y reduced it to non-bonding at the sacrifice of the Cu–O bond. The Cu–Cu overlap population for a neutral Cu_2O layer (28 electrons per unit cell) is 0.02, indicating a non-bonding Cu–Cu contact (Fig. 1(d), dashed line). Thus Cu_2O layer is a stable, closed-shell unit, with a Fermi level of -12.9 eV. Fig. 2 shows how the energy changes as a function of the distance of the oxygen atom from the Cu plane. Both the neutral (28 electrons per unit cell) and a positively charged Cu_2O prefer the planar square geometry. Addition of electrons to the layer, however, can cause the oxygen atom to shift out of the plane, as the total energy of the system is lowered. This is because as the oxygen atoms move out of the

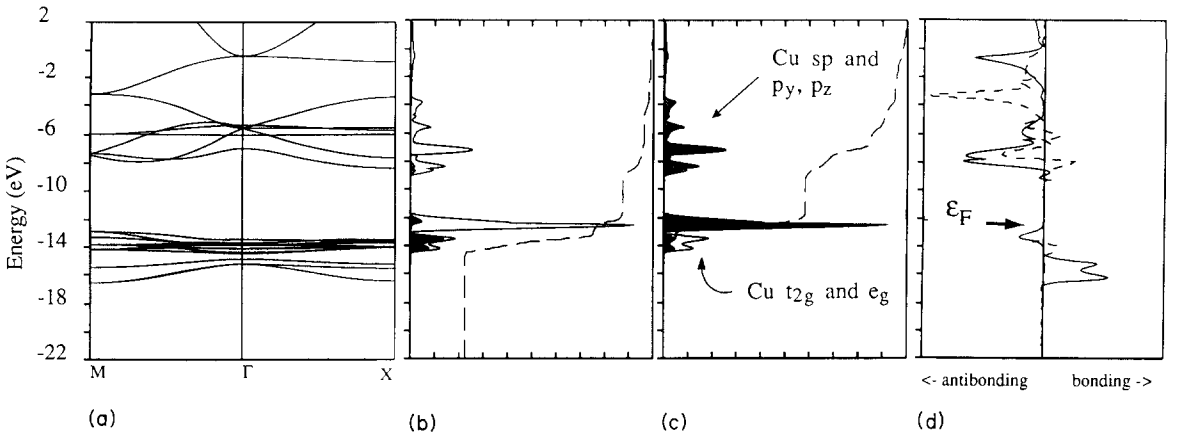

Fig. 1. Band structure (a), oxygen in Cu_2O (b) and Cu in Cu_2O (c) contributions to the total density of states, and the COOP curves of the Cu–O (solid line) and Cu–Cu bonds (dashed line) in the two-dimensional Cu_2O layer (d).

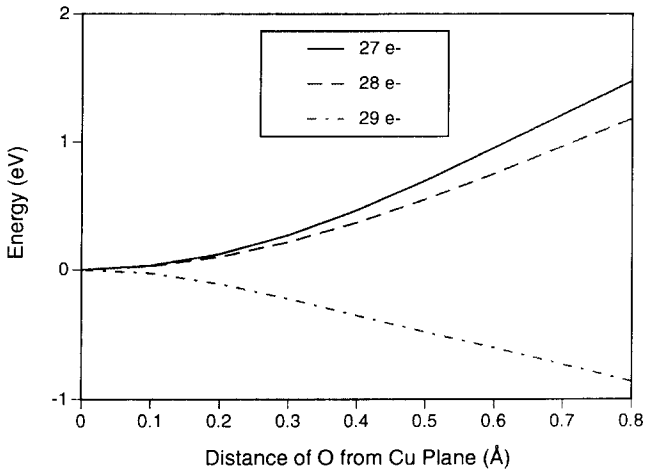

Fig. 2. Change of total energy as a function of the distance from the oxygen to the Cu plane in the two-dimensional Cu_2O layer. Twenty-eight electrons correspond to a neutral Cu_2O layer.

plane, the stabilization to the oxygen orbitals indicated in **4** and **5** is lost.

3. The Cu_2Se_2 layer

The bonding pattern of this layer is closely related to that of the $BaAl_4$ structure and the borane compounds [13,25]. We formally assign the oxidation state of Cu as Cu^{+1}. If we ignore the closed-shell d^{10} block, then each Cu atom has four empty sp^3 hybrids. Thus in each hollow of the Cu square lattice there are four sp^3 hybrids pointing towards an apical Se atom. Each Se atom has p_x, $p_y$orbitals, and two sp hybrids, one pointing to the hollow (hy_{in}), and one pointing away from the hollow (hy_{out}). The basis functions are shown in **6**.

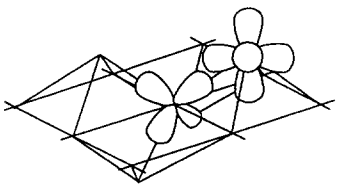

6

The four Cu hybrids in each hollow form four cyclobutadienoid symmetry-adapted molecular orbitals (see the left side of **7**). The a_1 orbital interacts with

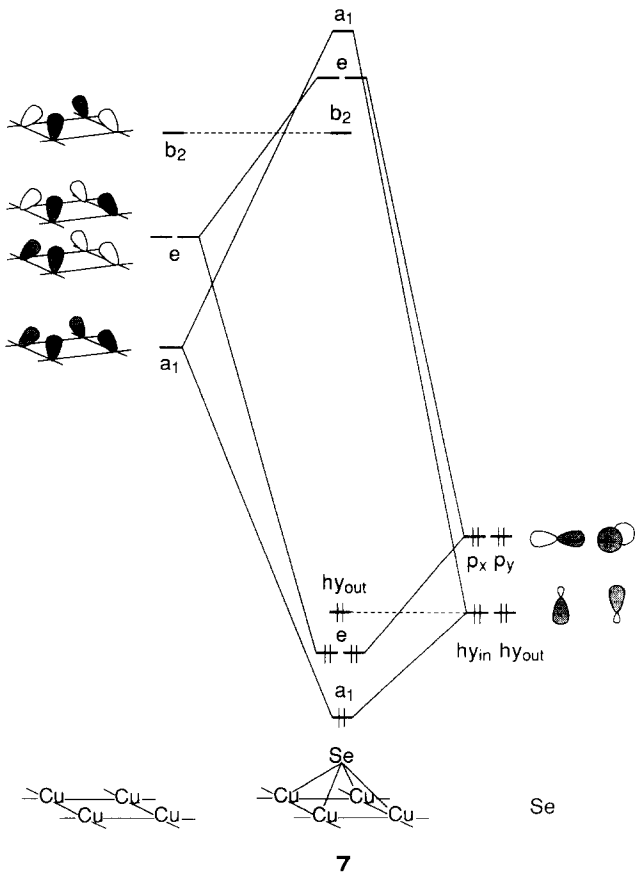

7

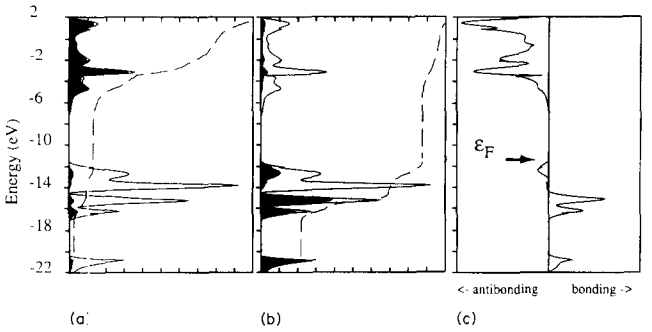

Fig. 3. Contributions to the total density of states from the Cu sp hybrids and p_y, p_z orbitals (a) and Se (b), and the COOP curves for the Cu–Se bond (c) in the Cu_2Se_2 layer.

Se hy_{in}, and e orbitals stabilize Se p_x and p_y. The hybrid orbital hy_{out} of Se is essentially non-bonding. Thus eight electrons per hollow filling the four Se orbitals give a closed-shell configuration. In other words, 16 electrons per Cu_2Se_2 unit plus another 20 electrons from the filled d orbitals of the two Cu^{+1} atoms correspond to the electron count of a semiconductor. A total of 36 electrons can be accommodated per Cu_2Se_2 unit (i.e. $Cu_2Se_2^{2-}$). The states below the Fermi level are mostly Cu–Se bonding and non-bonding, and above it, antibonding.

Fig. 3(a,b) shows the contribution of Se and Cu hybrids to the total density of states. The states above the Fermi level are nearly all Cu sp^3 hybrids. Fig. 3(c) is the Cu–Se COOP curve, showing that the states below the Fermi level have Cu–Se bonding and weakly antibonding characteristics. The Cu–Se overlap population is 0.27, indicating a strong bond. The Fermi level is −12.0 eV, higher than that of the Cu_2O layer (−12.9 eV). This is because each Cu atom interacts with more ligands in this layer, and the ligands (Se) are more electropositive than oxygen. Thus the d orbitals are pushed up more than in the Cu_2O layer, resulting in a higher Fermi level.

4. The $Na_{1.9}Cu_2Se_2Cu_2O$ structure

Having analyzed the bonding patterns of the separate layers, we can easily understand the electronic structure of the whole compound. Since there is only weak interaction between the layers, the total electronic structure is just the sum as the individual ones. Fig. 4 shows the COOP curves of Cu–O and Cu–Se bonds in the three-dimensional crystal. Indeed, they resemble those of the individual layers in Figs. 1 and 3. The DOS plots, which are not shown, are also simply the addition of DOS of the individual layers. From the analysis of the DOS and COOP curves, we can also say that the Na layer merely acts as electron donors, and does not participate in the interlayer covalent bonding.

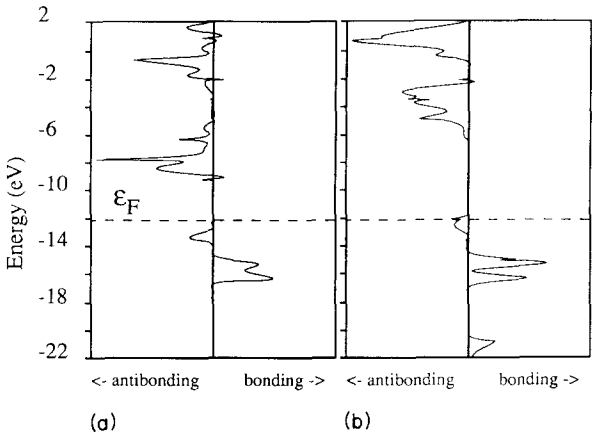

Fig. 4. The COOP curves for the Cu–O (in $Na_{1.9}Cu_2Se_2Cu_2O$) (a) and Cu–Se (in $Na_{1.9}Cu_2Se_2Cu_2$) (b) bonds in the three-dimensional $Na_{1.9}Cu_2Se_2Cu_2O$ structure.

Since the Fermi level in the Cu_2Se_2 layer is higher, removing electrons from the solid will result in lowering the number of electrons in this layer. In other words, the holes should reside in this layer. Thus the Cu_2Se_2 layer is the conduction layer, and Na and Cu_2O are the charge reservoir layers.

5. Conclusions

In this contribution we have analyzed the electronic structure of the $Na_{1.9}Cu_2Se_2Cu_2O$ solid. In this compound, the Cu atom has a d^{10} electronic configuration. A related family of compounds first synthesized in Schäfer's group, $A_2Mn_2X_2O_2Mn$ (A = Sr, Ba; X = P, As, Sb, Bi) [26], possess the same structural type, but the O_2Mn layer is an anti-Cu_2O type in which the oxygen is linearly coordinated to two Mn atoms, and Mn is squarely coordinated to four oxygen atoms. A formal electron count such as $(Ba^{2+})_2(Mn^{2+})_2$-$(P^{3-})_2(O^{2-})_2(Mn^{2+})$ gives a d^5 electronic configuration at the transition metal center. Recently, Stetson and Kauzlarich have measured the magnetic properties of these compounds [27]. The magnitude of the magnetic susceptibility indicates that the Mn atom is in a high spin state. Thus the analysis for a d^{10} transition metal can be applied to the high spin d^5 Mn, because in the latter, all d orbitals are occupied, albeit with only one electron. The geometry of a square-coordinated d^{10} transition metal is common. In light of this and of the above analysis, the electronic structure of the $A_2Mn_2X_2O_2Mn$ family can also be understood.

The Na deficiency in $Na_{1.9}Cu_2Se_2Cu_2O$ might be a result of the flux reaction condition. Since excessive Se was used, it is possible that a small amount of Na diffused into the Se melt. It would be interesting to confirm the existence of the holes in this compound by experimental means, such as by the Hall or thermal power coefficient determination.

Acknowledgment

We thank Professor Roald Hoffmann of Cornell University for very valuable discussions. This work has been supported in part by NSF through the PYI program (CHE-91-57717) and by the Donors of the Petroleum Research Fund administered by the American Chemical Society. Part of the computations were carried out at the National Center for Supercomputing Applications at University of Illinois at Urbana-Champaign.

Appendix

The extended Hückel tight-binding method was used in the calculations [28–31]. The extended Hückel parameters are listed in Table 1. The oxidation state of Cu is not sensitive to the parameters used, as a shift of the orbital energy by 1 eV upwards or downwards resulted in a change of charge on Cu by about 0.2 electron. The actual geometry of the crystal was applied ($a = 3.914$ Å, $c = 21.623$ Å) [5]. A set of 108 k points was generated according to the method of Pack and Monkhorst [32].

Table 1
Extended Hückel parameters

Orbital	H_{ii} (eV)	ζ_1	ζ_2	c_1	c_2
Cu 4s	−11.4	2.2			
4p	−6.06	2.2			
3d	−14.0	5.95	2.30	0.5933	0.5744
O 2s	−32.3	2.275			
2p	−14.8	2.275			
Se 4s	−20.5	2.44			
4p	−14.4	2.07			
Na 3s	−5.1	1.000			
3p	−3.0	1.000			

References

[1] H.W. Weber (ed.), *High-T_c Superconductors*, Plenum, New York, 1988.
[2] G.R. Stewart, *Rev. Mod. Phys., 56* (1984) 755.
[3] T. Kasuya and T. Saso (eds.), *Theory of Heavy Fermions and Valence Fluctuations*, Springer-Verlag, New York, 1985.
[4] C. Zheng and R. Hoffmann, *J. Am. Chem. Soc., 108* (1986) 3078.
[5] Y. Park, D.C. DeGroot, J.L. Schindler, C.R. Kannewurf and M.G. Kanatzidis, *Chem. Mater., 5* (1993) 8.
[6] K.M. Merz and R. Hoffmann, *Inorg. Chem., 27* (1988) 2120.
[7] A.L. Bowman, T.C. Wallace, J.L. Yarnell and R.G. Wenzel, *Acta Crystallogr., 21* (1966) 843.
[8] A.F. Wells, *Structural Inorganic Chemistry*, 5th edition, Oxford University Press, New York, 1987.
[9] R.E. McCarley, *Philos. Trans. R. Soc. London Ser. A, 308* (1982) 141.
[10] R.E. McCarley, *ACS Symp. Ser., 211* (1983) 273.
[11] K. Lii, R.E. McCarley, S. Kim and R.A. Jacobson, *J. Solid State Chem., 64* (1986) 347.
[12] R.J. Cava, B. Batlogg, J.J. Krajewski, L.W. Rupp, L.F. Schneemeyer, T. Siegrist, R.B. vanDover, P. Marsh, W.F. Peck, P.K. Gallagher, S.H. Galrum, J.H. Marshall, R.C. Farrow, J.V. Waszczak, R. Hull and P. Trevor, *Nature, 336* (1988) 211.
[13] C. Zheng and R. Hoffmann, *Z. Naturforsch., B41* (1986) 292.
[14] G. Savelsberg and H. Schäfer, *Z. Naturforsch., B33* (1978) 370.
[15] Y. Jiang, S. Alvarez and R. Hoffmann, *Inorg. Chem., 24* (1985) 749.
[16] J. Buckingham (eds.), *Dictionary of Organometallic Compounds*, Chapman and Hall, New York, 1984.
[17] C. Janiak and R. Hoffmann, *Inorg. Chem., 28* (1989) 2743.
[18] G. Wilkinson, F.G. A. Stone and E.W. Abel (eds.), *Comprensive Organometallic Chemistry*, Pergamon Press, New York, 1981.
[19] K. Takahashi and H. Tanino, *Chem. Lett.,* (1988) 641.
[20] R. Restori and D. Schwarzenbach, *Acta Crystallogr., Sect. B, 42* (1986) 201.
[21] H. Effenberger, *Acta Crystallogr. Sect. C., 47* (1991) 2644.
[22] P. Sherwood and R. Hoffmann, *Inorg. Chem., 28* (1989) 509.
[23] J.R. Rambo, J.C. Huffman and G. Christou, *J. Am. Chem. Soc., 111* (1989) 8027.
[24] J.K. Burdett and T. Hughbanks, *J. Am. Chem. Soc., 106* (1984) 3101.
[25] W.N. Lipscomb, *Boron Hydrides*, W.A. Benjamin, New York, 1963.
[26] E. Brechtel, G. Cordier and H. Schäfer, *Z. Naturforsch., B34* (1979) 777.
[27] N.T. Stetson and S.M. Kauzlarich, *Inorg. Chem., 30* (1991) 3969.
[28] R. Hoffmann and W.N. Lipscomb, *J. Chem. Phys., 36* (1962) 2179.
[29] R. Hoffmann and W.N. Lipscomb, *J. Chem. Phys., 37* (1962) 2872.
[30] R. Hoffmann, *J. Chem. Phys., 39* (1963) 1397.
[31] M.-H. Whangbo, R. Hoffmann and R.B. Woodward, *Proc. R. Soc. London Ser. A, 366* (1979) 23.
[32] J.D. Pack and H.J. Monkhorst, *Phys. Rev. B, 16* (1977) 1748.